

An elastic metamaterial with simultaneously negative mass density and bulk modulus

X. N. Liu,^{1,2} G. K. Hu,² G. L. Huang,^{1,a)} and C. T. Sun³

¹Department of Systems Engineering, University of Arkansas at Little Rock, Little Rock, Arkansas 72204, USA

²School of Aerospace Engineering, Beijing Institute of Technology, Beijing 100081, People's Republic of China

³School of Aeronautics and Astronautics, Purdue University, West Lafayette, Indiana 47907, USA

(Received 18 March 2011; accepted 12 May 2011; published online 21 June 2011)

In this letter, an elastic metamaterial which exhibits simultaneously negative effective mass density and bulk modulus is presented with a single unit structure made of solid materials. The double-negative properties are achieved through a chiral microstructure that is capable of producing simultaneous translational and rotational resonances. The negative effective mass density and effective bulk modulus are numerically determined and confirmed by the analysis of wave propagation. The left-handed wave propagation property of this metamaterial is demonstrated by the negative refraction of acoustic waves. © 2011 American Institute of Physics.

[doi:10.1063/1.3597651]

In 1967, Veselago theoretically investigated a visionary material with simultaneously negative permittivity and permeability.¹ This material is termed as a left-handed material (LHM). The concept did not become a reality until 2001 when Shelby *et al.*² proposed designs of structured materials with microstructures of metallic wires and split-ring resonators.^{3,4} The LHM leads to many unusual characteristics: negative refraction, reversed Doppler effect, reversed Cerenkov radiation, and superlensing for applications in information and communication technologies.⁵⁻⁷

In the same time, there has been also a great interest to design elastic/acoustic (EA) metamaterials. The EA metamaterial was experimentally demonstrated through the localized resonance structure constructed by coating a heavy sphere with soft silicone rubber which is then encased in epoxy.⁸ On the other hand, Fang *et al.*⁹ designed an acoustic metamaterial by using an array of subwavelength Helmholtz resonators. Bipolar and monopolar local resonances were later proved to be the essential wave mechanisms for producing negative effective mass density (NMD) and negative effective bulk modulus (NBM) of the metamaterial, respectively. Various EA metamaterial designs of solid and fluid unit mixture were proposed to obtain simultaneously NMD and NBM.¹⁰⁻¹³ However, the aforementioned designs all require the combined use of solid and fluid media and are difficult to fabricate. Furthermore, the resulting frequency band for double-negative properties is usually narrow. Recently an experiment of ultrasonic focusing was reported by Zhang *et al.*,¹⁴ who construct a fluid LHM using a planar network of subwavelength Helmholtz resonators. However, a practical double-negative EA metamaterial made purely from solid materials is still absent.

In this letter, we propose a double-negative EA metamaterial which can be achieved with solid materials. In the proposed EA metamaterial, the effective NBM is achieved by a chiral microstructure. To illustrate the concept, we consider a

one-dimensional (1D) chiral mass-spring unit shown in Fig. 1(a). Four mass-less springs and a rigid disk with rotational inertia I are pin-connected. The two springs with spring constant k_2 are tangential to the disk with an angle α . The pin joints A, B, and C are kept in the horizontal axis. The rotation of the disk is induced by equally applied force F . For infinitesimal deformation, the force in the spring k_2 is given by $f_2 = k_2(R\theta - x \cos \alpha)$. The dynamic motion of the disk of radius R is then governed by $2f_2R = -I\partial^2\theta/\partial t^2$. The balance of forces at pin joint A gives $F = k_1x - f_2 \cos \alpha$. By assuming time-harmonic quantities, i.e., $(F, x, \theta) = (\hat{F}, \hat{x}, \hat{\theta})e^{i\omega t}$, eliminating θ and defining the dynamic effective stiffness k_{eff} of the system by $\hat{F} = k_{\text{eff}}(2\hat{x})$, we have

$$k_{\text{eff}} = \frac{k_1}{2} + \frac{k_2(\cos \alpha)^2}{2} \left(1 - \frac{\omega_0^2}{\omega_0^2 - \omega^2} \right), \quad (1)$$

where $\omega_0 = \sqrt{2k_2R^2/I}$ is the rotational resonance frequency. Equation (1) reveals that k_{eff} becomes negative in the fre-

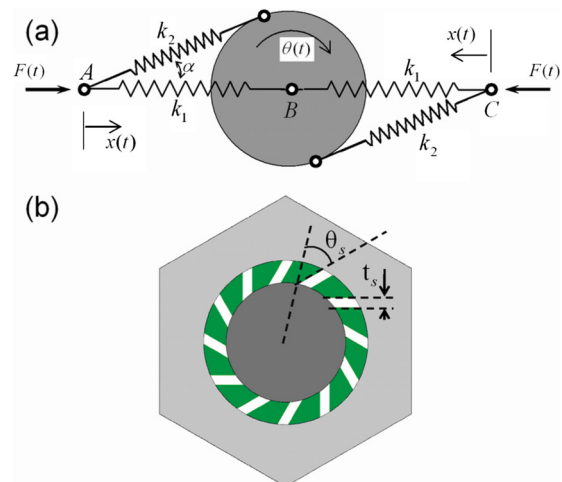


FIG. 1. (Color online) (a) 1D representative mass-spring model; (b) the unit cell of the 2D metamaterial made from solid media. The unit cell is composed of three-component continuum media by a chirally soft-coated heavy cylinder core embedded in matrix.

^{a)}Author to whom correspondence should be addressed. Electronic mail: glhuang@ualr.edu.

quency range $\sqrt{k_1/(k_1+k_2 \cos^2 \alpha)} < \omega/\omega_0 < 1$. Since the translation resonance of the disk can be used to generate the effect of NMD, it is conceivable that the chiral microstructure may produce both NMD and NBM at a common frequency. Based on the discrete model of Fig. 1(a), a practical continuum two-dimensional (2D) metamaterial is proposed and its unit cell (representative volume element) is depicted in Fig. 1(b). The unit cell is based on the 2D analogy of the well-known three-component sonic crystal,⁸ i.e., soft-coated heavy cylinder core embedded in a matrix. A number of (n_s) slots with width t_s are cut out from the coating material. The slots are equispaced in azimuth and oriented at an angle θ_s with respect to the radial direction. The periodic structure is arranged in a triangular lattice with lattice constant a . It is known that the dispersion relations for elastic metamaterials with triangular lattices are isotropic near the Γ point in the wave vector space.^{15,16} The unit structure lacks any planes of mirror symmetry and, thus, it is said to be chiral.¹⁷ It is known that the traditional three-component metamaterial without chirality gives NMD because of the translational resonance of the core. However, the rotational resonance can never be excited because of the mirror symmetry. By introducing chirality, rotational resonance may be coupled to produce the overall dilatation of the unit cell. As a result, NBM could be obtained. With an appropriate design of the unit cell, we anticipate to achieve both types of resonance in the overlapped frequency range and hence the double negativity.

Due to the geometric complexity, the use of analytical methods^{10,18} for solving the dynamic response of the 2D EA metamaterial is not practicable. Instead, a numerical method is suggested to determine the effective properties of the proposed 2D metamaterial. Under the long wavelength assumption, the global stress, strain, resultant force and acceleration of the unit cell can be obtained by averaging local quantities on the *external* boundary as

$$\begin{aligned} \Sigma_{\alpha\beta} &= \frac{1}{V} \int_{\partial V} \sigma_{\alpha\gamma} x_{\beta} ds_{\gamma}, & E_{\alpha\beta} &= \frac{1}{2V} \int_{\partial V} (u_{\alpha} ds_{\beta} + u_{\beta} ds_{\alpha}), \\ F_{\alpha} &= \frac{1}{V} \int_{\partial V} \sigma_{\alpha\beta} ds_{\beta}, & \ddot{U}_{\alpha} &= \frac{1}{S} \int_{\partial V} \ddot{u}_{\alpha} ds, \end{aligned} \quad (2)$$

respectively, where $\alpha, \beta, \gamma = 1, 2$, $\sigma_{\alpha\beta}$, u_{α} , and \ddot{u}_{α} are the local stress, displacement, and acceleration fields, respectively, $ds_{\alpha} = n_{\alpha} ds$ with n_{α} being the boundary unit normal, x_{α} is position vector, and V and ∂V denote unit cell's volume and external boundary. Considering the macroscopic isotropy, the effective bulk, shear modulus and mass density for the 2D problem can be defined as

$$K_{\text{eff}} = \frac{1}{2} \Sigma_{\alpha\alpha} / E_{\alpha\alpha}, \quad \mu_{\text{eff}} = \frac{1}{2} \Sigma'_{\alpha\beta} / E'_{\alpha\beta}, \quad \rho_{\text{eff}} = F_{\alpha} / \ddot{U}_{\alpha}, \quad (3)$$

where $\Sigma'_{\alpha\beta}$ and $E'_{\alpha\beta}$ mean the deviatoric parts of the global stress and strain, respectively. The local displacement field can be assumed as $\hat{u}_{\alpha}(\mathbf{x}) = \hat{u}_{\alpha}^0 + \hat{E}_{\alpha\beta} x_{\beta}$, where the displacement field \hat{u}_{α} is compatible with a given macrostrain tensor $\hat{E}_{\alpha\beta}$ plus a given rigid translation u_{α}^0 . To obtain the local fields, the time-harmonic displacement is applied on the unit cell's boundary ∂V as $u_{\alpha}(x, t) = \hat{u}_{\alpha}(x) e^{i\omega t}$. The problem is solved by using the finite element method (FEM) with frequency swept over the interested range, from which the global stress and force can be determined based on Eq. (2). In

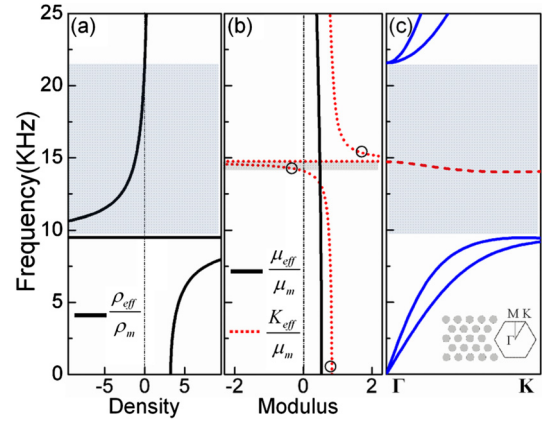


FIG. 2. (Color online) (a) Effective dynamic density, (b) bulk modulus, and (c) band structure of the elastic metamaterial. The predicted overlapped NMD and NBM frequency range matches the negative pass band in the band diagram which is highlighted by dashed line.

the numerical example, epoxy, lead, and low-density polyethylene are chosen to be the materials of matrix, core, and coating, respectively.¹⁹ The core is 5.6 mm in diameter and the coating thickness is 0.7 mm. The triangular lattice constant is $a = 10.75$ mm. The slot parameters are $n_s = 12$, $t_s = 0.4$ mm, and $\theta_s = 56^\circ$. Figure 2(a) shows normalized effective mass density ρ_{eff}/ρ_m as a function of wave frequency, where ρ_m is the density of the epoxy. It is seen that the NMD occurs in the range of 9.51–21.54 kHz. Figure 2(b) shows the normalized bulk modulus K_{eff}/μ_m and shear modulus μ_{eff}/μ_m as a function of frequency, where μ_m is the shear modulus of the epoxy. It is of interest to note that K_{eff} becomes negative in the frequency range of 14.08–14.72 kHz while μ_{eff} is always positive. Further, in the range of 14.30–14.72 kHz both effective longitudinal modulus $E_{\text{eff}} = K_{\text{eff}} + \mu_{\text{eff}}$ and effective mass density ρ_{eff} become negative. Thus, it is a pass band in which the left-handed wave propagation behavior is implied. To demonstrate this, the band structure calculation is performed by using the FEM in conjunction with the Bloch's theorem.²⁰ The wave dispersion relation along ΓK direction is shown in Fig. 2(c). The lattice array and the Brillouin zone are plotted in the inset of Fig. 2(c). A stop band is observed for both longitudinal and transverse wave branches in the frequency range of 9.44–21.58 kHz which perfectly matches the frequency range of the predicted NMD. In addition, a new pass band with negative slope is found in the frequency range of 14.05–14.73 kHz which lies close to the overlapped region of the NMD and negative longitudinal modulus. A discrepancy in band width between the pass band and the double-negative properties prediction may be attributed to the following reasons: (1) the applied boundary condition does not take into account of phase change across the unit cell and is accurate only in the long wave limit, thus the negative band and the double-negative properties matches better at upper bound and (2) for the chiral metamaterial, when the rotational resonance of the core occurs, the global stress would become asymmetric and the classical theory of elasticity cannot fully characterize this material. The higher-order continuum theories may be more suitable for this application.²¹

To clearly demonstrate the mechanism of NBM, the deformation states corresponding to three typical values of the K_{eff} are plotted in Fig. 3, which are highlighted in Fig. 2(b) by circle dots. In these figures, undeformed unit cells are

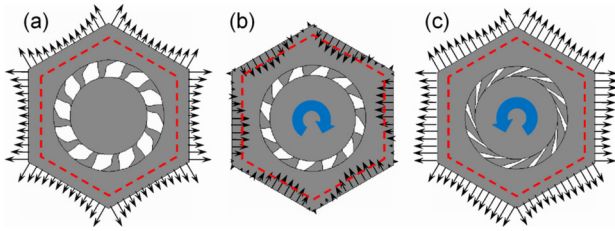


FIG. 3. (Color online) Deformation and rotational resonance states corresponding to three typical values of the effective dynamic bulk modulus: (a) quasistatic value; (b) negative value; and (c) positive peak. The frequency points are highlighted by circle dots in Fig. 2(b).

shown in dashed lines, and the boundary tractions are also depicted by arrows. In Fig. 3(a) (0 kHz), quasistatic K_{eff} is obtained because the frequency is far away from the core rotational resonance frequency. As shown Fig. 3(b), when the frequency (14.5 kHz) approaches the rotational resonance frequency from below, the core rotates in-phase with the overall deformation so that a very large clockwise rotation is generated in conjunction with an expanded unit cell. Such a rotation causes a compression state in the matrix and external boundary resulting in the NBM. In Fig. 3(c), when the frequency (15.2 kHz) approaches the rotational resonance frequency from above, the anticlockwise core rotation enhances the tension state in the matrix and, consequently, a positive peak of dynamic effective modulus occurs.

The most prominent phenomenon related to double-negative metamaterials is the negative refraction. In order to test this, we perform a large scale full wave simulation consists of detailed microstructure using commercial finite element code COMSOL. We take a 30.0° wedged sample which consists of 546 unit cells with a triangular array immersed in water (1000 kg/m^3 in density, 1500 m/s in sound speed). A Gaussian acoustic pressure beam is launched in the fluid from the bottom side of the wedge. The acoustic pressure (hydrostatic stress) fields in the system are plotted in Fig. 4(a) at frequency 14.53 kHz, where the effective bulk, shear modulus and mass density of the metamaterial are calculated to be -1.58 GPa , 0.42 GPa , and -1481 kg/m^3 , respectively. It can be clearly seen that the energy flux of the refraction wave outside of the sample travels on the negative refraction side of the surface normal in the range of the double-negative pass band. Upon closer observation of the wave pattern of the hydrostatic stress field inside the solid wedge, the “back-wave” phenomenon inside the metamaterial is clearly seen. Figure 4(b) shows the acoustic pressure (hydrostatic stress) field in a left-sloped wedge with the same chirality in Fig. 4(a) at frequency 14.53 kHz. It is interesting to notice that the almost same negative refraction phenomenon can be observed as that in Fig. 4(a) although the mirror symmetry of the two metamaterials is broken due to the chirality. This agreement further substantiates the fact that the isotropic effective medium with simultaneously NBM and NMD associated with the coupled translational and rotational resonances are still valid to explain the negative refraction mechanism.

In summary, we have demonstrated that acoustic metamaterials with double-negative mass and modulus properties can be constructed with solid materials. The double-

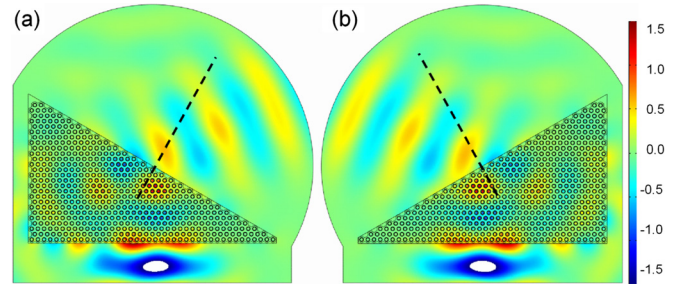


FIG. 4. (Color online) Numerical simulation of negative refraction. The intensity of pressure field in fluids and hydrostatic stress in solids for incidence and refraction are shown in different colors. (a) Right-sloped wedge at 14.53 kHz frequency. (b) Left-sloped wedge at 14.53 kHz frequency.

negative properties are obtained by utilizing simultaneously the local translational and rotational resonances of a chiral microstructure. The proposed design is scalable and relatively easy to fabricate and hence is hopeful for possible experimental validations.

This work was supported in part by Air Force Office of Scientific Research under Grant No. AF 9550-10-0061 with Program Manager Dr. Byung-Lip (Les) Lee and NSF EA-GER Program No. 1037569 with Program Manager Dr. Clark Cooper and in part by National Natural Science Foundation of China under Grant Nos. 10972036 and 10832002.

- ¹V. G. Veselago, *Sov. Phys. Usp.* **10**, 509 (1968).
- ²R. A. Shelby, D. R. Smith, and S. Schultz, *Science* **292**, 77 (2001).
- ³J. B. Pendry, A. J. Holden, D. J. Robbins, and W. J. Stewart, *IEEE Trans. Microwave Theory Tech.* **47**, 2075 (1999).
- ⁴D. R. Smith, W. J. Padilla, D. C. Vier, S. C. Nemat-Nasser, and S. Schultz, *Phys. Rev. Lett.* **84**, 4184 (2000).
- ⁵J. B. Pendry, *Phys. Rev. Lett.* **85**, 3966 (2000).
- ⁶N. Engheta and R. W. Ziolkowski, *IEEE Trans. Microwave Theory Tech.* **53**, 1535 (2005).
- ⁷C. Luo, M. Ibanescu, S. G. Johnson, and J. D. Joannopoulos, *Science* **299**, 368 (2003).
- ⁸Z. Y. Liu, X. Zhang, Y. Mao, Y. Y. Zhu, C. T. Chan, and P. Sheng, *Science* **289**, 1734 (2000).
- ⁹N. Fang, D. J. Xi, J. Y. Xu, M. Ambrati, W. Sprituravanich, C. Sun, and X. Zhang, *Nature Mater.* **5**, 452 (2006).
- ¹⁰Y. Q. Ding, Z. Y. Liu, C. Y. Qiu, and J. Shi, *Phys. Rev. Lett.* **99**, 093904 (2007).
- ¹¹J. Li and C. T. Chan, *Phys. Rev. E* **70**, 055602 (2004).
- ¹²K. Deng, Y. Q. Ding, Z. J. He, H. P. Zhao, J. Shi, and Z. Y. Liu, *J. Appl. Phys.* **105**, 124909 (2009).
- ¹³Y. Wu, L. Yun, and Z. Q. Zhang, *Phys. Rev. B* **76**, 205313 (2007).
- ¹⁴S. Zhang, L. Yin, and N. Fang, *Phys. Rev. Lett.* **102**, 194301 (2009).
- ¹⁵Y. Wu and Z. Q. Zhang, *Phys. Rev. B* **79**, 195111 (2009).
- ¹⁶Q. Ni and J. Cheng, *Phys. Rev. B* **72**, 014305 (2005).
- ¹⁷R. Lakes, *Int. J. Mech. Sci.* **43**, 1579 (2001).
- ¹⁸G. W. Milton and J. Willis, *Proc. R. Soc. London, Ser. A* **463**, 855 (2007).
- ¹⁹The material parameters are $\rho=1.11 \times 10^3 \text{ kg/m}^3$, $K=3.14 \times 10^9 \text{ Pa}$, and $\mu=0.89 \times 10^9 \text{ Pa}$ for unfilled epoxy resin; $\rho=0.92 \times 10^3 \text{ kg/m}^3$, $K=0.57 \times 10^9 \text{ Pa}$, and $\mu=0.13 \times 10^9 \text{ Pa}$ for low-density Polyethylene,²² and $\rho=11.6 \times 10^3 \text{ kg/m}^3$, $K=52.6 \times 10^9 \text{ Pa}$, and $\mu=14.9 \times 10^9 \text{ Pa}$ for lead.²³ Here, ρ , K , and μ denote density, bulk moduli, and shear moduli, respectively.
- ²⁰X. N. Liu, G. K. Hu, C. T. Sun, and G. L. Huang, *J. Sound Vib.* **330**, 2536 (2011).
- ²¹A. C. Eringen, *Microcontinuum Field Theories I: Foundations and Solids* (Springer, New York, 1999).
- ²²C. E. S. Selector 4.0 <http://www.grantadesign.com/products/ces/>.
- ²³C. Kittel, *Introduction to Solid State Physics*, 3rd ed. (Wiley, New York, 1966).